A New Organic Nanoporous Architecture: Dumb-Bell-Shaped Molecules with Guests in Parallel Channels

Torsten Müller,[a] Jürg Hulliger,*[b] Wilhelm Seichter,[a] Edwin Weber,*[a] Thomas Weber,[c] and Michael Wübbenhorst[d]

Abstract: A new type of dumb-bell-shaped host molecule (**6**–**8**) has been synthesised, of which 1,8-bis((1)-adamantyl)-1,3,5,7-octatetrayne (**8** = BAOT) forms an open porous architecture when cocrystallised with a number of typical solvent molecules. Adamantyl substituents attached to a tetraalkyne spacer build up the walls of parallel channels wherein guest molecules are aligned. Surprisingly, the tetraalkyne unit is significantly bent. Desolvation experiments provide evidence for a reversible inclusion of guests. In the case of the inclusion of 2-butanone, a partial substitution by symmetrical and asymmetrical long-chain chromophores during crystallisation was possible. Stained crystals showed optical frequency doubling. The crystal structure analysis revealed a centric space group, although considerable translational and orientational disorder was present. Application of scanning pyroelectric microscopy revealed that the growth of inclusion compounds with 2-butanone produced polar ordering of guest molecules, which were aligned in two macro-domains of opposing polarity. The resulting orientation of the carbonyl dipoles is in agreement with the theoretical prediction of a Markov model of spontaneous polarity formation based on molecular recognition processes on growing crystal faces. The present case represents a new example of a property-driven supramolecular synthesis.

Keywords: inclusion compounds · NLO properties · oligoalkynes · open-framed structures · scanning pyroelectric microscopy · supramolecular chemistry

Introduction

Synthetic inorganic zeolites[1] are classical examples of nanoporous materials; however, recently a variety of organic network architectures[2] and inclusion compounds[3] featuring typical properties of nanoporous materials have been described.[4] Crystal engineering[5] and principles of molecular tectonics[6] have focussed on overcoming the difficulties inherent in the design of *open-framed* organic structures.[7] However, many attempts have produced crystal structures showing the interpenetration of two or more sublattices, driven by close-packing requirements.[8] In these structures, the open space is filled up by solvent molecules, which are difficult to remove or to substitute without structural disintegration. *Interpenetration* is hence considered a main difficulty in the design of nanoporous materials containing, for example, parallel channels capable of hosting a variety of functional guest molecules.

Confining close-packed, functionalised molecules within parallel channels allows one to address a number of interesting solid-state properties, especially when the guests themselves are aligned co-parallel within the cavities.[9] More recent examples include a model system for light-harvesting by migration of photonic energy along aligned dye molecules in a zeolite,[10] the demonstration of an organic laser using a zeolite host,[11] and the tuning of spontaneous polarity formation in organic channel-type inclusion compounds driven by a Markov process.[12]

Because many of the chromophores providing photonic and nonlinear optical (NLO) properties can be made from rod-shaped molecules, the design of disc- (oblate-top) or rod- (prolate-top) shaped host molecules is of interest for assembling corresponding guest and host compounds into channel-type supramolecular structures. A particular class of host molecules which may be suited for this purpose are dumb-bell-type entities[13] (Scheme 1).

---

[a] Prof. Dr. E. Weber, Dr. W. Seichter, T. Müller
Institut für Organische Chemie, TU Bergakademie Freiberg
Leipziger Strasse 29, D-09596 Freiberg/Sachsen (Germany)
Fax: (+49) 3731-393170
E-mail: weber@tu-freiberg.de

[b] Prof. Dr. J. Hulliger
Department of Chemistry and Biochemistry, University of Berne
Freiestrasse 3, CH-3012 Berne (Switzerland)
Fax: (+41) 31 631-3993
E-mail: juerg.hulliger@iac.unibe.ch

[c] Dr. T. Weber
Laboratory of Crystallography, University of Berne
Freiestrasse 3, CH-3012 Berne (Switzerland)

[d] Dr. M. Wübbenhorst
Department of Polymer Technology, Delft University of Technology
P.O. Box 5045, NL-2600 GA Delft (The Netherlands)

0947-6539/00/0601-0054 $ 17.50+.50/0

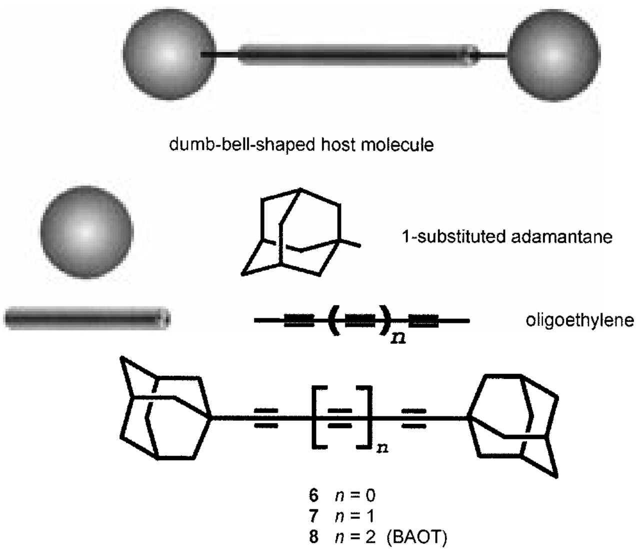

Scheme 1. Schematic representations of the new host molecules.

Here we report the synthesis of a new type of host molecule featuring a dumb-bell shape. Initial results on the structure and polar properties of 1,8-bis((1)-adamantyl)-1,3,5,7-octatetrayne (**8** = BAOT), which forms channel-type inclusion crystals with various solvent molecules, are presented. In the case of 2-butanone, some of the solvent can be substituted by long-chain NLO active molecules (see Table 1).

Results and Discussion

Synthesis of the dumb-bell-shaped host molecule: The starting material **1** was synthesised from 1-bromoadamantane and vinyl bromide in the presence of aluminium bromide as catalyst, followed by double dehydrobromination with potassium hydroxide in dimethyl sulfoxide.[14] Reaction of **1** with 2-(trimethylsilyl)ethynyl bromide (**2**), obtained from bis(trimethylsilyl)ethyne (**2a**), yielded the protected 1-(1,3-butadiynyl)adamantane (**3**).[15] Cleavage of the silyl group of **3** gave the terminal butadiyne **4**. A Cadiot-Chodkiewicz procedure between **5** (from **1**) and **4** led to the unsymmetrical dumb-bell-shaped molecule **7**.[16] Coupling of **1** or **4** by a Eglington reaction[17] gave the symmetrical compounds **6**[14a] or **8** (BAOT) (Scheme 2).

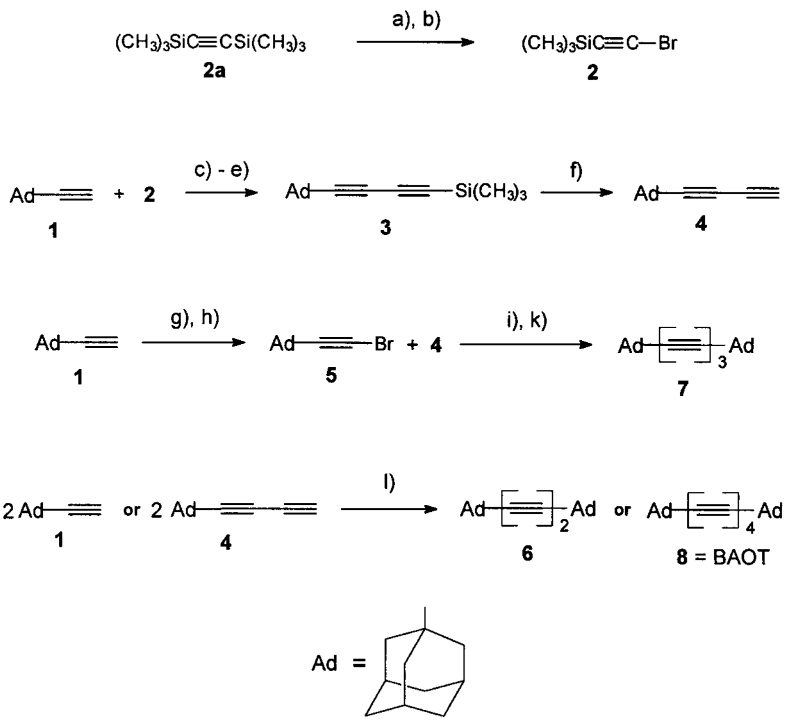

Scheme 2. Synthesis of compounds **6**–**8**. a) 0 °C, MeLi/LiBr; b) −70 °C, pyridine, bromine; c) −70 °C, *n*BuLi; d) 0 °C, $Cu^{I}Br$; e) pyridine, **2**, 50 °C; f) 25 °C, $KF \cdot 2H_2O$; g) −75 °C, *n*BuLi; h) −50 °C, bromine, diethyl ether; i) $Cu^{I}Br$, $NH_2OH \cdot HCl$, 50 % aqueous ethylamine, reflux; k) 35 °C, **5**, methanol; l) $Cu(OAc)_2$, methanol, pyridine, reflux.

Inclusion formation with solvents: Crystallisation of BAOT (**8**) from solvents such as 2-butanone, (±)-2-bromobutane, *n*-hexane, tetrahydrofuran, toluene and cyclohexanol yielded inclusion compounds showing for example a host–guest ratio of 1:1 in the case of 2-butanone (BU). Using well developed single crystals of BAOT/BU, BAOT/cyclohexanol[18] and BAOT/(()-2-bromobutane[19], we were able to determine the crystal structures.

In the case of BU and (±)-2-bromobutane guests, a channel-type packing of BAOT was found, featuring two types of channels (Figure 1): Oval channels having a maximum cross-section as large as 9.8 Å containing guest molecules and smaller ones remaining empty. The channels including BU also show characteristic narrowings with a minimum diameter of 4.2 Å.[20] The inner surface of both types of channels consists of adamantane units and ethynyl chain fragments facing each other. A further remarkable feature of this structure is that the tetrayne spacer in BAOT shows a strong deviation from linearity of the ethynyl units (total bending angle: 14.6°), which is probably caused by packing effects rather than by the electronic structure of the host molecule.[21] As far as we know, there is no structure in the literature showing a similar distortion of the ethynyl units from linearity apart from cycloalkynes. The distribution of the intensities of measured reflections reflected a centre of symmetry for the packing of BAOT molecules. Within the large channels, the BU guest molecules showed translational and rotational disorder.

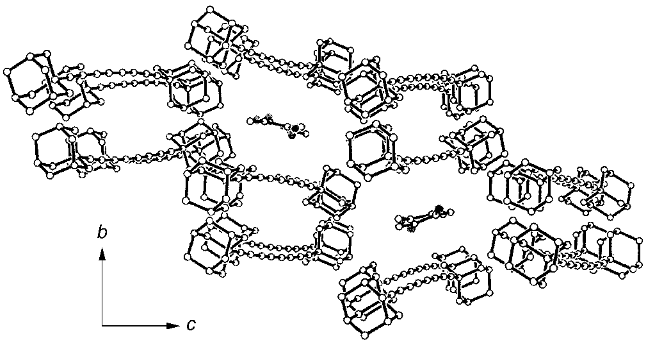

Figure 1. X-ray structure of the inclusion compound BAOT/BU viewed along the *a* axis (channel direction). Note the bending of the tetraethyne spacer. 2-Butanone molecules are disordered, resulting in a nonpolar space group; however, scanning pyroelectric microscopy revealed a polar packing, resulting in twinned crystals.

Both the inclusion structures containing BU or (±)-2-bromobutane are monoclinic featuring a similar metric. In the case of cyclohexanol, the larger guest molecule leads to an expansion of the structure, which may by described by layered packing.[18] Thermogravimetry and differential scanning calorimetry revealed that 2-butanone and (±)-2-bromobutane desorb continuously when powders were heated from 25–150 °C in open air. Up to 150 °C, no significant thermal signal appeared; however, when the sample was heated further to 190 °C, an endothermic peak (≈4 kJ mol^{-1}) was indicative of a structural change. This is supported by temperature-dependent powder X-ray measurements that show a significant change of cell parameters in the range of 180–190 °C.

The fact there is no observable change in the powder diffraction pattern during desorption of the guest molecules leads to an important question: Are the channels in the lattice framework of BAOT stable without the presence of guest molecules such as BU or (±)-2-bromobutane? Although the channels might contract in some way, the basic architecture of BAOT seems to still exist. However, a lack of solvent-free single crystals that are suitable for an X-ray analysis study has so far prevented the structural differences between BAOT/BU and BAOT to be determined.

Further evidence supporting an open porous structure showing reversible inclusion was obtained from a vapour phase treatment[22] of BAOT(s) with BU(v) at two temperatures: At 25 °C only part of the total amount of BAOT was loaded after 30 min (overall BAOT/BU ratio of about 20:1), whereas at 80 °C (1.2 bar BU) for 5 h, a ratio of 2:1 was much closer to the composition obtained by crystallisation from BU (1:1).[23]

Co-inclusion of dye molecules: Inclusion of guest compounds capable of electronic functions into the channel matrix of BAOT may provide interesting materials with respect to fields mentioned in the introduction. Along this line, co-crystallisation of BAOT with BU and crocetin dialdehyde (**9**), 2-(2,6,11,15-tetramethyl-16-oxo-hexadeca-2,4,6,8,10,12,14-heptaenylidene)malononitrile (**10**) or *trans-β*-APO′-8-carotenal (**11**) (Table 1) was carried out, resulting in homogeneously coloured crystals showing a pronounced dichroism (Figure 2). Based on a compositional analysis by optical spectroscopy, **9** and **11** are included to an approximate ratio of 14:1 and 80:1 (BU/dye), respectively. For the guest **10**, no defined ratio was observed. An interesting finding is that apart from the inclusion compound with BU, coloured crystals were not obtained with any other solvents, regardless of whether or not they formed an inclusion compound with BAOT. This particular type of co-inclusion seems to be a specific structural property of the channel matrix of BAOT/BU crystals.

Table 1. Co-included rod-shaped dyes, their inclusion ratio and space group of the corresponding BAOT/BU-dye lattice.

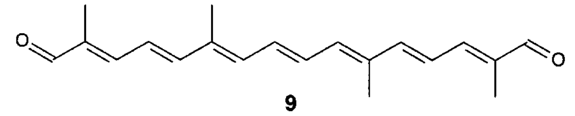

9

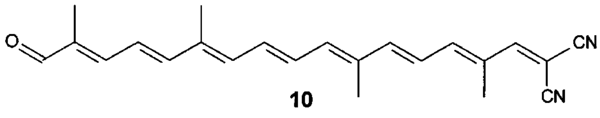

10

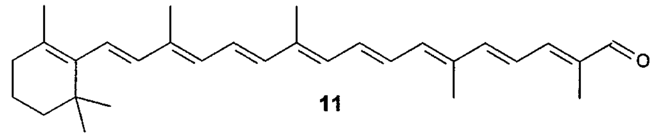

11

	SHG of inclusion compound	Space group determined by X-ray	Host/dye ratio measured by VIS
9	–	$P2_1/n$(centric)	14/1
10	+	–	no defined ratio
11	+	P_n (noncentric)	80/1

The crystal structures of BAOT/BU-**9** and BAOT/BU-**11** were determined by X-ray structure analysis. In both struc-

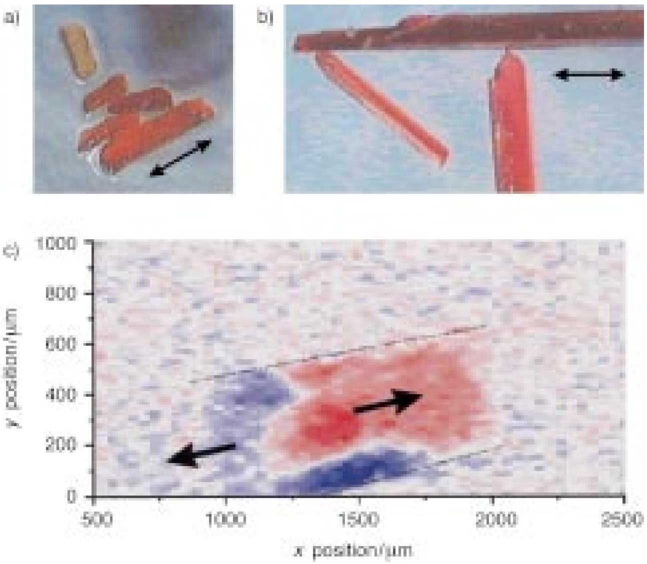

Figure 2. Pronounced dichroism of a) BAOT/BU-**9** and b) BAOT/BU-**10**, seen by polarised light. The needle axis of crystals represents the direction of the channels. c) Pyroelectric measurement (SPEM) of BAOT/BU: *x*,*y* scan of the surface of a needle-like crystal (*x* nearly parallel to the needle axis). Thin black lines indicate the needle shape. Red colour: polarisation vector in the +*x* (→) direction; blue colour: −*x* (←), correspondingly. The red and blue domain interpenetrate, owing to the growth of the crystal. The intensity of the colour is a measure of the local net polarity. Because of a rather weak signal, there is some noise around the sample, which on average does not give rise to polarisation.

tures the BAOT molecules form a centric packing. Nevertheless, in BAOT/BU-**11** the BU molecules preferentially undergo polar ordering (space group P_n) (Figure 3). Although the channel-type architecture was confirmed in the case of both co-inclusions, the guests **9** and **11** could not be located. Information on i) the alignment of the long axis of **9**–**11**, and ii) a preferred orientation of dipoles was obtained from the observation of i) the dichroism (Figure 2) and ii) a second harmonic generation (SHG) effect of both BAOT/BU-**11** and BAOT/BU-**10**. Note, that polar ordering of BU molecules cannot give rise to the observed SHG response, because the hyperpolarisability of BU is orders of magnitude lower than for **10** or **11**. The SHG can therefore be attributed to a polar ordering of **10** or **11** in the channels of BAOT/BU.

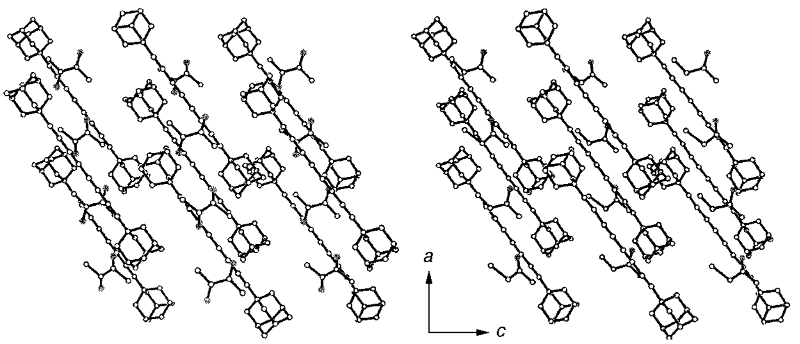

Figure 3. Crystal structures of BAOT/BU-**9** (left) showing the alignment of disordered 2-butanone molecules under the influence of symmetrical guest **9** and BAOT/BU-**11** (right) with BU molecules undergoing polar ordering.

At this point of the analysis it became evident that scanning pyroelectric microscopy (SPEM) might be a useful technique to elude more details of the structure of BAOT-BU crystals. SPEM has been previously applied to the analysis of $AlPO_4$-5 loaded with NLO guest molecules,[24] and to inclusion compounds of perhydrotriphenylene.[25] This new technique provides local information on the pyroelectric properties of a material by scanning the surface with a laser heat source focused to a probing spot size of about $10 \times 10\ \mu m^2$. According to this analysis (Figure 2c) BAOT/BU crystals represent a *polar* host–guest material: i) as grown crystals consist of mainly two macro-domains, wherein the resultant polarisation is of opposite orientation; ii) part of all BU guests show uniform ordering of their dipoles giving rise to a macroscopic polarisation, seen when measuring the pyroelectric effect. iii) A further important result of the analysis of the pyroelectric effect is that we established that the carbonyl groups of BU preferentially are oriented towards the capping faces of needle-shaped crystals.

From Figure 1 it follows that the BU guest molecules are aligned in channels along the *a* axis located in two crystallographically different positions A and B. A Weissenberg X-ray photograph of the zeroth layer perpendicular to the needle axis revealed that its layer is spanned by the reciprocal axes *b** and *c**. Thus, the *a* axis and therefore the channels are parallel to the needle axis. The angles between the dipole moment of the carbonyl group of molecules at sites A or B and the needle axis are 4° and 19°, respectively (Figure 4).

The polar ordering of BU in the channels of BAOT/BU can be understood on the basis of a general principle of polarity formation applied to crystal lattices containing dipolar species.[26] If there is a non-vanishing energy difference between the BU–BU interaction along each channel, that is if there is a difference in the energy of the $-CH_3\cdots H_3C$- and $R_2C{=}O\cdots O{=}CR_2$ interactions, then polarity evolution during crystal growth (not necessarily during nucleation) into two macro-domains becomes possible (Markov process). Because the molecular recognition of $R_2C{=}O\cdots O{=}CR_2$ is destabilising in nature, theory predicts that the oxygen atom of the carbonyl group will be oriented towards the crystal–nutrient interface. This basic feature was confirmed by SPEM.[25] However, the extent of polarity may be small, and the polar ordering of BU within the channels does not require a polar packing of host molecules. In our case, the BAOT molecules pack in a centric manner.

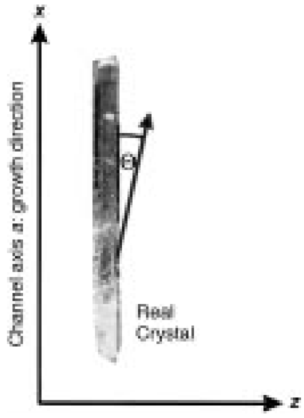

Figure 4. Relative orientation of molecular dipoles $R_2C{=}O$ (→: dipole direction) of two crystallographically different sites A and B occupied by 2-butanone guest molecules in BAOT/BU: $\Theta = 4°$, $\Theta = 19°$. As a result of the pyroelectric measurements, carbonyl groups are oriented towards the growing interface.

When a second functional component (**9**, **10**, **11**) is present, we can apply arguments put forward for BU: In the case of **10**, functional group interactions of terminal groups such as a dicyano group may be stronger when interacting with BU, than interactions of BU with itself. Although we can understand polar ordering of **9** and **10**, it remains open as to why polar ordering of BU is found for BAOT/BU-**11**.

Conclusions

The synthesis of an oligoalkyne-based dumb-bell-shaped molecule has produced a new type of channel-forming host–guest compound wherein solvent molecules could partially be replaced by long-chain chromophores. The packing behaviour of the adamantyl entity linked by tetraalkyne spacers seems to overcome the problem of *interpenetrating networks*, a typical structural feature of many organic supramolecular assemblies.[8]

An unusual bending of the -[-C≡C-]$_4$- chain may be indicative of some stress contributing to the total energy of the lattice. Although the host–guest ratio is fixed, the crystal structure analysis of, for example, BAOT/BU has encountered considerable difficulties in localising the guest molecules, owing to significant translational and particularly 180° orientational disorder. This means, along the channel axis, BU molecules show a distribution of their dipolar moment with respect to a 180° rotation. Similar phenomena have been observed for other channel-type inclusion compounds.[27] The present system is a new example of a host–guest assembly, in which guest molecules are required to adapt either an ↑ or ↓ orientation of their dipoles when entering channels.[12] As discovered recently, such supramolecular solids fulfill the requirements for applying a general principle of polarity formation,[26] showing that polarity can *develop* along a crystal growth process. With regard to property-directed supramolecular chemistry, we have here a new case of a synthetic principle in which a physical property develops while the compound is formed during crystallisation. Importantly, in this new approach, design of a property (here polarity) does not rely on what property a seed crystal will have: the property *polarity* can *evolve* as the crystal grows, reaching a constant state after a certain number of attachments.

The X-ray structure analysis of, for example, BAOT/BU would leave us with a *centric* packing of BU. In view of an wR_2 value of 0.2575 we cannot retrieve the real structure of such crystals only from X-ray data. Complementary techniques are necessary. In this respect, scanning pyroelectric microscopy (SPEM) can provide space-resolved (μm scale) information on the polarity of orientationally disordered lattices. Following the analysis of the pyroelectric effect, we can conclude that BAOT/BU crystals consist (ideally) of two adjacent macro-domains (in real cases often overlapping[28]) showing an opposite net polarisation. As reported in detail for inclusion compounds of perhydrotriphenylene,[9] application of a homogeneous Markov process is sufficient to explain polarity formation during crystal growth, that is the attachments of dipoles to sites where guest molecules have already entered the channel structure. In the case of BU, a non-vanishing energy difference between ($R_2C{=}O\cdots O{=}CR_2$) and ($R{-}CH_3\cdots H_3C{-}R$) is sufficient to give rise to a certain evolution of polarity as crystals grow along their channel axis. In this most simple model, no assumptions on co-operative phenomena of ordering enter the description of the polarity evolution. As a result, grown crystals are not in the global F minimum, although differences are generally expected to be small ($|\Delta F| = |F_{\text{thermodynamic}} - F_{\text{growth}}| \leq \approx 1\,\text{kJ}\,\text{mol}^{-1}$).

Surprisingly, the co-inclusion of **11** led to an increased degree of the polar ordering of BU (acentric space group P_n), whereas **9** did not remove the centre of symmetry. In fact, we have to be careful in trusting details of the X-ray structure analysis, because of rather large wR_2 values for both **9** and **11**. From a theoretical analysis of the molecular recognition of X-π-X and X-π-Y or Y-π-Y (-X⋯X-: destabilising interaction, -Y⋯Y-, -X⋯Y-: weak stabilising interactions, respectively) molecules confined to interact collinearly, we know that X-π-X can enhance the polar ordering of X-π-Y when added during the growth. In contrast, addition of Y-π-Y may even cancel polarity when present in the nutrient.[12b] Up to now, it is not clear to which family the aldehyde group in **9**–**11** belongs. Clearly, the dicyano groups of **10** are X substituents, however, the aldehyde in **9**–**11** may belong to X or Y, depending on the hydrogen-bonding when confined to interact collinearly, as given by the channel geometry. Following the analysis of a large number of solid-state synthons in organic crystal structures, the collinear aldehyde–aldehyde interaction is not a well reported motif.[5b] However, in the Cambridge Structural Data Base a few examples of aldehyde–aldehyde motifs are present. In the case where X is $R_2C{=}O$, then BAOT/BU-**9** crystals should show an enhanced pyroelectric effect in comparison to BAOT/BU.[12b] Further experiments along this lines are in progress.

A second interesting property of this new type of channel-forming host molecule (BAOT = **8**) is its potential ability to form an open framework structure that seems to show a reversible release of BU.

Future synthetic work will concentrate on the modification of moieties to be attached to the oligoalkyne spacer. By using the bicyclo[2.2.2]octyl substituent, we aim to investigate the role of the adamantyl entity in the channel formation. Furthermore, bicyclo[2.2.2]octyl is C_3 symmetric, which may give rise to another packing of channels if appropriate elongated guest molecules are used. Finally, we will attempt to include chromophores showing pronounced electronic and optical properties into a channel frame mediating some lateral π⋯π interactions between guests and host molecules. This is interesting with respect to photoconductivity and the possibility of investigating optical storage properties by photorefraction.[29]

Experimental Section

General methods: Melting points were determined on a Büchi 510 and were not corrected. NMR spectra were recorded on a Bruker Avance DPX 400 spectrometer with Me_4Si or $CHCl_3$ (in $CDCl_3$) as internal standard at 25 °C with 400 MHz for ^1H NMR and 100 MHz for ^{13}C NMR. Mass spectra were recorded on a Varian MAT 2/2 mass spectrometer under electrospray conditions.

All reactions were monitored by thin-layer chromatography (TLC) carried out on Merck silica gel 60 F_{254} coated plates with UV light, iodine, concentrated sulfuric acid and heat as developing agents. Merck silica gel (60, particle size 0.063–0.1 mm) and sephadex LH-20 were used for column chromatography. Dry tetrahydrofuran, diethyl ether, and pentane were distilled from sodium/benzophenone, dichloromethane and toluene from calcium chloride, pyridine from calcium oxide, methanol from magnesium and 2-butanone (BU) from potassium permanganate. Bromine was dried with concentrated sulfuric acid immediately prior to use.

Diethylamine, dimethyl sulfoxide and *N*,*N*-dimethylformamide were used p.a. (Merck). Bis(trimethylsilyl)acetylene (**2a**) and *trans*-*β*-APO′-8-carotenal (**11**) were obtained from Aldrich. We thank Prof. H. P. Pfander for a few grams of crocetindialdehyde (**9**). The other reagents were purchased from Fluka, Lancaster and Merck. All reactions were carried out under an argon atmosphere. Yields refer to chromatographically and spectroscopically (^{1}H NMR) homogenous materials.

2-(Trimethylsilyl)ethynyl bromide (2): A solution of methyllithium/lithium bromide in diethyl ether (1.5 M, 100 mL, 0.15 mol) at 0 °C was added dropwise to a solution of **2a** (23.8 g, 0.14 mol) in tetrahydrofuran (200 mL). Stirring was continued at 0 °C for 30 min and then at room temperature for 30 min. After cooling the mixture to −70 °C, pyridine (22.8 mL, 0.28 mol) and bromine (8 mL, 0.15 mol), dissolved in dichloromethane (20 mL), were added. The mixture was stirred for 30 min, allowed to warm to room temperature and poured into ice-cold hydrochloric acid (6 M, 50 mL) and extracted with ice-cold *n*-pentane (3 × 50 mL). The organic layer was separated and washed with ice-cold 6 M HCl (3 × 25 mL), followed by aqueous solutions of 20 % $CdCl_2$, saturated NaCl, saturated Na_2SO_4, saturated $NaHCO_3$ and saturated NaCl, in this sequence, dried over $MgSO_4$ and filtered. Evaporation of the solvent and vacuum distillation yielded a pale brown, clear liquid (19.1 g, b.p. 55–70 °C (140 mbar). This fraction containing a mixture of **2** and the starting material (75:25) was used without further purification. MS (EI, 70 eV): *m/z* (%): 176 (3), 163 (100), 133 (10), 109 (9), 97 (13).

1-(4-Trimethylsilyl-1,3-butadiynyl)adamantane (3): To a solution of **1**[14] (1.6 g, 10 mmol) in THF (20 mL) was added dropwise a solution of butyllithium (1.8 M, 5.5 mL, 10 mmol) at −70 °C. Then copper(I) bromide (1.4 g, 10 mmol) was added at 0 °C and the mixture was stirred for 30 min at 25 °C. The solvent was removed in vacuo at ambient temperature to give a yellow solid, which was taken up in pyridine (20 mL). After **2** (1.8 g, 10 mmol) was added, the mixture was stirred at 50 °C for 1 h. The resulting brown solution was poured into ice-cold HCl (6 M, 50 mL) and extracted with *n*-hexane (3 × 30 mL). The combined organic layers were washed with HCl (6 M, 2 × 25 mL) and saturated aqueous solutions of $NaHCO_3$ and NaCl, dried over Na_2SO_4, and filtered. Evaporation of the solvent in vacuo and purification of the solid residue by column chromatography (silica gel, *n*-hexane) yielded **3** as a colorless solid: 1 g (4 mmol, 42 %); m.p. 125–135 °C; ^{1}H NMR: $\delta = 0.2$ (br., 9H; $SiCH_3$), 1.7 (br., 6H; $CHCH_2C$), 1.9 (br., 6H; $CHCH_2CH$), 2.0 (br., 3H; CH_2CHCH_2); ^{13}C NMR: $\delta = -0.3$, 27.6, 30.1, 36.1, 42.1, 66.6, 84.3, 88.4; MS (EI, 70 eV): *m/z* (%): 256 (15), 241 (100).

1-(1,3-Butadiynyl)adamantane (4): A mixture of **3** (3.6 g, 14 mmol) and potassium fluoride dihydrate (1.7 g, 18 mmol) in *N,N*-dimethylformamide (50 mL) was stirred for 1 h at 25 °C. The suspension was poured into HCl (3 M, 50 mL) and extracted with *n*-hexane (3 × 50 mL). The combined organic solutions were washed with HCl (3 M, 2 × 15 mL) and saturated aqueous solutions of $NaHCO_3$ and NaCl, dried over Na_2SO_4 and filtered. Evaporation of the solvent (heating was avoided) and purification of the residual brown oil with column chromatography (silica gel, *n*-hexane) yielded **4** as white solid: 2.4 g (13 mmol, 93 %); ^{1}H NMR: $\delta =$ 1.6 (br., 6H; $CHCH_2C$), 1.9 (br., 6H; $CHCH_2CH$), 2.0 (br, 3H; CH_2CHCH_2); ^{13}C NMR: $\delta = 27.9$, 29.9, 36.2, 42.0, 65.7, 66.6, 68.5; MS (EI, 70 eV): *m/z* (%): 184 (100), 169 (11), 155 (25), 141 (60), 128 (56), 115 (45), 91 (35), 79 (43).

2-(1-Adamantyl)ethynyl bromide (5): A solution of butyllithium (1.8 M, 5.5 mL, 10 mmol) at −75 °C was added dropwise to a solution of **1**[14] (1.6 g, 10 mol) in diethyl ether (50 mL). The mixture was stirred for 1 h and then allowed to warm to −50 °C. Bromine (1.9 g, 12 mmol), dissolved in diethyl ether (5 mL), was added and the solution was allowed to warm to room temperature. After water was added (50 mL), the layers were separated and the aqueous layer was extracted with diethyl ether (3 × 50 mL). The combined organic solutions were dried over Na_2SO_4 and filtered. Evaporation of the solvent yielded **5** as a brownish solid. No further purification was done: 2.2 g (9 mmol, 92 %); MS (EI, 70 eV): *m/z* (%): 241 (3), 238 (23), 159 (100), 131 (14), 117 (23).

1,4-Bis(1-adamantyl)-1,3-butayne (6): A solution of **1**[14] (1.0 g, 6.4 mmol) and copper(II) acetate (1.8 g, 10 mmol) in methanol/pyridine (50 mL, 1:1) was refluxed for 6 h. The mixture was cooled to 0 °C and poured carefully into concentrated HCl (100 mL). *n*-Hexane (50 mL) was added to the resulting suspension, the layers were separated, and the aqueous solution was extracted with *n*-hexane (4 × 50 mL). The combined organic layers were washed with water, 1 M HCl, and water, dried over Na_2SO_4, and filtered. The solvent was removed in vacuo to yield a brownish solid residue, which was purified by column chromatography on silica gel (*n*-hexane). Recrystallisation from 2-butanone gave colourless crystals: 0.3 g (1 mmol, 31 %); m.p. 338–340 °C; ^{1}H NMR: $\delta = 1.6$ (br., 12H; $CHCH_2C$), 1.8 (br., 12H; $CHCH_2CH$), 1.9 (br., 6H; CH_2CHCH_2); ^{13}C NMR: $\delta = 27.8$, 30.1, 36.2, 42.4, 64.1, 86.0, MS (EI,70 eV): *m/z* (%): 318 (100), 275 (36), 261 (30), 135 (34); $C_{24}H_{30}$ (318.5): calcd C 90.57, H 9.43; found C 90.45, H 9.32.

1,6-Bis(1-adamantyl)-1,3,5-hexatriyne (7): To a solution of **4** (1.5 g, 8 mmol) in methanol (50 mL) was added copper(I) bromide (0.2 g) and hydroxylamine hydrochloride (0.5 g) both dissolved in 50 % aqueous ethylamine (16 mL) at room temperature. The mixture was refluxed for 30 min, then cooled to 35 °C and **5** (2 g, 8 mmol), dissolved in methanol (20 mL), was added. Further stirring of the mixture for 5 h yielded a suspension, which was poured into water (50 mL) and extracted with diethyl ether (3 × 50 mL). The combined organic layers were dried over Na_2SO_4 and filtered. Evaporation of the solvent yielded a brownish solid mixture of products (**7** contaminated with **6** and **8**). Purification by column chromatography on silica gel (*n*-hexane), followed by chromatography on sephadex (dichloromethane) and recrystallisation from 2-butanone gave **7** as pale yellow crystals: 1.4 g (4 mmol, 49 %); m.p. 237–241 °C, ^{1}H NMR: $\delta = 1.7$ (br., 12H; $CHCH_2C$), 1.9 (br., 12H; $CHCH_2CH$), 2.0 (br., 6H; CH_2CHCH_2); ^{13}C NMR: $\delta = 27.7$, 30.2, 36.1, 42.1, 61.6, 64.7, 86.6; MS (EI, 70 eV): *m/z* (%): 342 (100), 318 (11), 299 (7); $C_{26}H_{30}$ (342.5): calcd C 91.18, H 8.82, found C 90.82, H 8.84.

1,8-Bis(1-adamantyl)-1,3,5,7-octatetrayne (8): The same procedure as for **6** was applied but **4** was used instead of **1**. Purification by column chromatography on silica gel (*n*-hexane) and on sephadex (dichloromethane) followed by re-crystallisation from 2-butanone gave pale yellow, transparent crystals: 1.1 g (3 mmol, 91 %); m.p. 217–219 °C; ^{1}H NMR: $\delta =$ 1.7 (br., 12H; $CHCH_2C$), 1.9 (br., 12H; $CHCH_2CH$), 2.0 (br., 6H; CH_2CHCH_2), ^{13}C NMR: $\delta = 28.0$, 30.7, 36.5, 42.3, 62.0, 62.3, 65.2, 87.6; MS (EI, 70 eV): *m/z* (%): 366 (100), 323 (2), 318 (6); $C_{28}H_{30}$(366.5): calcd C 91.75, H 8.25, found C 91.25 , H 8.29.

2-(2,6,11,15-tetramethyl-16-oxo-hexadeca-2,4,6,8,10,12,14-heptaenylidene)-malononitrile (10): A solution of crocetin dialdehyde (**9**) (1.75 mmol, 0.52 g), malononitrile (1.4 mmol, 90 mg), β-alanine (0.2 mmol, 15 mg), and acetic acid (0.02 mL) in toluene (30 mL) was refluxed for 3 h.[30] Molecular sieves (Riedel-deHaen, 0.4 nm, pearl-shaped, grain-size ca. 2 mm) were present in the flask to remove the reaction water. After the mixture had been cooled to room temperature, it was washed with saturated aqueous NaCl solution (4 × 25 mL). The organic layer was dried over $CaCl_2$ and filtered. Evaporation of the solvent and purification by chromatography on silica gel (*n*-hexane/dichloromethane, 1:3) yielded **10** as a deep red solid: 0.27 g (0.8 mmol, 45 %), m.p. 229–234 °C; MS (EI, 70 eV): *m/z* (%): 344 (100), 147 (16), 119 (13).

Crystallisation: BAOT (**8**) (10 mg) and guest compounds **9**–**11** (2 mg) were dissolved in 2-butanone (BU) (2 mL) using ultrasound and if necessary under heating. The solutions were combined on a crystallisation dish and the solvent was evaporated under argon flow at isothermal conditions ($T =$ 22.5 °C).[31] Crystals of BAOT/BU (**9**–**11**) form as red (**9**, **11**) and dark red (**10**) needles. They show a dichroism, appearing yellowish (**9**, **11**) or colourless (**10**) when illuminated with light-polarised perpendicular to the needle axis.

X-ray crystallography: Single crystals of the inclusion compounds BAOT/BU, BAOT/BU-**9**, and BAOT/BU-**11** were obtained from controlled and isothermal evaporation from 2-butanone.[31] Crystal data were collected with a CAD-4 diffractometer (Enraf-Nonius) equipped with a graphite monochromator. The intensity of three control reflections measure after every 250 reflections did not change significantly over X-ray exposure for 90 h. Unit cell dimensions and standard deviations were obtained by a least-squares fit to 25 reflections. The data were collected for Lorentz and polarisation effects. The structure was solved by direct methods with SHELX-86. All carbon and oxygen atoms were refined anisotropically by the full-matrix least-squares method. Hydrogen atoms were included in the ideal positions with a fixed isotropic U value of 0.08 Å^2. All calculations were performed on a Silicon Graphics Iris Indigo 6R2 XS workstation using programs HELENA (data reduction), SHELXL-93 (refinement) and PLATON (plotting). BAOT/BU: crystal size: $0.40 \times 0.40 \times 0.40$ mm^3; crystal system: monoclinic; space group: $P2_1/n$; unit cell dimensions: $a =$ 11.431(12), $b = 12.308(6)$, $c = 18.291(14)$ Å, $\beta = 101.11(8)°$; $T = 178(2)$ K;

$\lambda = 0.71073$ Å; $V = 2525.2(35)$ Å^3; $Z = 4$; $F(000) = 952$; $\rho_{calcd} = 1.154$ g cm^{-3}; absorption coefficient: 0.067 mm^{-1}; Θ range for data collection: 1.95 to 29.95°; scan type: ω - 2Θ; index ranges: $0 \leq h \leq 16$, $0 \leq k \leq 17$, $-25 \leq l \leq 25$; reflections collected: 7311; independent reflections: 3282 ($R_{int} = 0.0364$); refinement method: full-matrix least-squares on F^2: 1.059; R indices [$I > 2\sigma(I)$]: $R1 = 0.1046$, $wR_2 = 0.2575$; goodness of fit: 1.281. Weighting scheme: $w = 1/[\sigma^2(F_o^2) + (0.1016P)^2 + 3.8870P]$, where $P = (F_o^2 + 2F_c^2)/3$. Largest difference: peak and hole: 0.34 and -0.26 eA^{-3}.

BAOT/BU-**9**: crystal size: $0.20 \times 0.20 \times 0.15$ mm^3; crystal system: monoclinic; space group: $P2_1/n$; unit cell dimensions: $a = 11.454(1)$, $b = 12.327(1)$, $c = 18.310(2)$ Å, $\beta = 100.73(1)$°; $T = 178(2)$ K; $\lambda = 1.54178$ Å; $V = 2540.1(4)$ Å^3; $Z = 4$; $F(000) = 944$; $\rho_{calcd} = 1.142$ g cm^{-3}; absorption coefficient: 0.505 mm^{-1}; Θ range for data collection: 4.23 to 74.71°; scan type: ω - 2Θ; index ranges: $0 \leq h \leq 14$, $0 \leq k \leq 15$, $-22 \leq l \leq 22$; reflections collected: 5214; independent reflections: 3858 ($R_{int} = 0.0125$); refinement method: full-matrix least-squares on F^2: 1.149; R indices [$I > 2\sigma(I)$]: $R1 = 0.0819$, $wR_2 = 0.2235$; goodness of fit: 1.149. Weighting scheme: $w = 1/[\sigma^2(F_o^2) + (0.1106P)^2 + 2.5499P]$, where $P = (F_o^2 + 2F_c^2)/3$. Largest difference: peak and hole: 0.67 and -0.34 eA^{-3}.

BAOT/BU-**11**: crystal size: $0.20 \times 0.20 \times 0.15$ mm^3; crystal system: monoclinic; space group: P_n; unit cell dimensions: $a = 1.471(9)$, $b = 12.366(6)$, $c = 18.300(16)$ Å, $\beta = 100.87(6)$°; $T = 178(2)$ K; $\lambda = 1.54178$ Å; $V = 2543.1(32)$ Å^3; $Z = 4$; $F(000) = 952$; $\rho_{calcd} = 1.146$ g cm^{-3}; absorption coefficient: 0.504 mm^{-1}; Θ range for data collection: 3.58 to 75.11°; scan type: ω - 2Θ; index ranges: $-14 \leq h \leq 10$, $-9 \leq k \leq 15$, $-22 \leq l \leq 22$; reflections collected: 5495; independent reflections: 3607 ($R_{int} = 0.0163$); refinement method: full-matrix least-squares on F^2: 1.289; R indices [$I > 2\sigma(I)$]: $R1 = 0.1123$, $wR_2 = 0.3346$; goodness of fit: 1.289. Weighting scheme: $w = 1/[\sigma^2(F_o^2) + (0.2218P)^2 + 2.6620P]$, where $P = (F_o^2 + 2F_c^2)/3$. Largest difference: peak and hole: 0.67 and -0.39 eA^{-3}.

Crystallographic data (excluding structure factors) for the structures reported in this paper have been deposited with the Cambridge Crystallographic Data Centre as supplementary publication no. CCDC 111488 and no. CCDC 112042. The crystal structures of BAOT/BU and BAOT/BU-**9** are identical. Copies of the data can be obtained free of charge on application to CCDC, 12 Union Road, Cambridge CB2 IEZ (fax: (+44)1223-336-033; e-mail: deposit@ccdc.cam.ac.uk).

Second harmonic generation (SHG) and pyroelectric measurements: Qualitative SHG measurements were performed with a Q-switched Nd:YAG Laser operating at 1064 nm. Fine-grain powder samples or some small single crystals of BAOT/BU-**10** and BAOT/BU-**11** showed intense emission of green light when compared to, for example, urea. The effect cannot be due to pure BAOT/BU, **10** and **11**, which showed no SHG activity.

The existence of a permanent polarisation in BAOT/BU crystals has been confirmed by spatially resolved measurements of the pyroelectric effect (SPEM). Needle-shaped crystals of BAOT/BU (length typically 2–3 mm) were coated with a thin black ink for heat absorption, and scanned with a focussed beam of a laser diode ($\lambda = 639$ nm, power < 5 mW). The beam diameter of ≈ 10 µm and the low modulation frequency of the laser intensity ($f = 1$ Hz) enabled probing the pyroelectric activity within at a lateral resolution of about 10×10 µm^2. Changes of the polarity of the pyroelectric current are indicative of an inversion of the polarisation and thus for the preferred direction of the included molecular dipoles. From the current sign and the assumption that the pyroelectric coefficient is negative we can derive that the carbonyl groups are oriented towards the capping faces of crystals.

UV measurement: As grown, inclusion crystals were washed with ethanol/BU (1/1). The dried material was weighed and dissolved in BU (20 mL). Measurements were carried out in quartz cells with 1 cm path lengths. A SPECORD M500 spectrophotometer (Zeiss, Germany) was used to collect background spectra of the solvent, the pure BAOT and of the solutions.

Thermogravimetric (TG) and differential scanning calorimetry (DSC) measurement: The thermal decomposition of the different inclusion compounds of BAOT was studied by means of a TG-DSC Mettler system (50, 25) using open aluminium crucibles, sample weights of about 8 mg, a linear heating rate of 5 K min^{-1} and nitrogen as purge gas for all measurements.

Acknowledgements

The authors would like to thank Prof. Dr. H.-B. Bürgi for the use of X-ray equipment, Dr. Karl Krämer for his work on the temperature-dependent powder diffraction and Dr. Jürgen Seidel for vapour sorption/desorption measurements. This work is part of the Graduate School Program (GRK 208) of the TU Bergakademie Freiberg supported by the Deutsche Forschungsgemeinschaft. T.M. is grateful for a scholarship from this organisation. E.W. also thanks the Fonds der Chemischen Industrie for financial support. Part of this work has received support by the Swiss National Science Foundation.

---

[1] a) W. M. Meier, D. H. Olson, *Atlas of Zeolite Structure Types*, 3rd ed., Butterworth Heinemann, London, **1992**; b) P. T. Tanev, J.-R. Butruille, T. J. Pinnavaia in *Chemistry of Advanced Materials: An Overview* (Eds.: L. V. Interrante, M. J. Hampden-Smith), Wiley-VCH, Weinheim, **1998**; c) C. B. Aakeröy, A. M. Beatty, D. S. Leinen, *Angew. Chem.* **1999**, *111*, 1932–1936; *Angew. Chem. Int. Ed.* **1999**, *38*, 1815–1819.

[2] a) P. J. Langley, J. Hulliger, *Chem. Soc. Rev.* **1999**, *28*, 279–291; b) P. Brunet, M. Simard, J. D. Wuest, *J. Am. Chem. Soc.* **1997**, *119*, 2737–2738; c) V. A. Russell, M. D. Ward, *Chem. Mater.* **1996**, *8*, 1654–1666.

[3] a) E. Weber in *Kirk-Othmer Encyclopedia of Chemical Technology, Vol. 14* (Ed.: J. I. Kroschwitz), 4th ed., Wiley, New York, **1995**, pp. 122–154; b) K. Endo, T. Ezuhara, M. Koyanagi, H. Masuda, Y. Aoyama, *J. Am. Chem. Soc.* **1997**, *119*, 499–505; c) K. Kobayashi, M. Koyanagi, K. Endo, H. Masuda, Y. Aoyama, *Chem. Eur. J.* **1998**, *4*, 417–424.

[4] a) V. Ramamurthy, D. F. Eaton, *Chem. Mater.* **1994**, *6*, 1128; b) G. A. Ozin, A. Kuperman, A. Stein, *Angew. Chem.* **1998**, *110*, 48–64; *Angew. Chem. Int. Ed.* **1998**, *37*, 46–62; c) F. M. Menger, T. Tsuno, G. S. Hammond, *J. Am. Chem. Soc.* **1990**, *112*, 1263–1264; d) G. Liu, J. Ding, *Adv. Mater.* **1998**, *10*, 69–71; d) W. Srisiri, T. M. Sisson, D. F. O'Brien, K. M. McGrath, Y. Han, S. M. Gruner, *J. Am. Chem. Soc.* **1997**, *119*, 4866–4873; e) R. C. Smith, W. M. Fischer, D. L. Gin, *J. Am. Chem. Soc.* **1997**, *119*, 4092–4093.

[5] a) A. Nangia, G. R. Desiraju in *Design of Organic Solids, Vol. 198* (Ed.: E. Weber), Springer, Berlin, **1998**, pp. 57–95; b) G. R. Desiraju, *Angew. Chem.* **1995**, *107*, 2541–2558; *Angew. Chem. Int. Ed.* **1995**, *34*, 2328–2361.

[6] D. Su, X. Wang, M. Simard, J. D. Wuest, *Supramol. Chem.* **1995**, *6*, 171–178.

[7] J. A. Swift, A. M. Pivorar, A. M. Reynolds, M. D. Ward, *J. Am. Chem. Soc.* **1998**, *120*, 5887–5894.

[8] S. R. Batten, R. Robson, *Angew. Chem.* **1998**, *110*, 1558–1595, *Angew. Chem. Int. Ed.* **1998**, *37*, 1460–1494.

[9] R. Hoss, O. König, V. Kramer-Hoss, U. Berger, P. Rogin, J. Hulliger, *Angew. Chem.* **1996**, *108*, 1774–1776; *Angew. Chem. Int. Ed. Engl.* **1996**, *35*, 1664–1666.

[10] N. Gfeller, S. Megelski, G. Calzaferri, *J. Phys. Chem. B* **1999**, *103*, 1250–1257.

[11] G. Ihlein, F. Schüth, D. Kraus, U. Vietze, F. Laeri, *Adv. Mater.* **1998**, *10*, 1117.

[12] a) J. Hulliger, P. Rogin, A. Quintel, P. Rechsteiner, O. König, M. Wübbenhorst, *Adv. Mater.* **1997**, *9*, 677; b) S. W. Roth, P. J. Langley, A. Quintel, M. Wübbenhorst, P. Rechsteiner, P. Rogin, O. König, J. Hulliger, *Adv. Mater.* **1998**, *10*, 1543–1546.

[13] F.Toda in *Comprehensive Supramolecular Chemistry, Vol. 6* (Eds.: J. L. Atwood, J. E. D. Davies, D. D. MacNicol, F. Vögtle, K. S. Suslick), Pergamon, Oxford, **1996**, pp. 465–516.

[14] a) H. Stetter, P. Goebel, *Chem. Ber.* **1962**, *95*, 1039; b) Q. B. Broxterman, H. Hogeveen, *Tetrahedron Lett.* **1986**, *27*, 1055–1058.

[15] J. A. Miller, G. Zweifel, *Synthesis* **1983**, 128.

[16] W. Chodkiewicz, P. Cadiot, *C. R. Hebd. Seances Acad. Sci.* **1959**, *248*, 116.

[17] G. Eglington, A. R. Galbraith, *J. Chem. Soc.* **1959**, 889.

[18] Crystallographic data (excluding structure factors) for the structure reported in this paper have been deposited with the Cambridge Crystallographic Data Centre as supplementary publication no. CCDC-119507. Copies of the data can be obtained free of charge on

application to CCDC, 12 Union Road, Cambridge CB2 1EZ, UK (fax: (+44) 1223-336-033; e-mail: deposit@ccdc.cam.ac.uk).

[19] Refinement of this crystal structure turned out to be very difficult and has not been completed yet.

[20] MOLMAP, L. J. Barbaur, unpublished computer program, **1993**.

[21] E. Weber, W. Seichter, B. Hess, G. Will, H.-J. Dasting, *J. Phys. Org. Chem.* **1995**, *8*, 94-96.

[22] D. Meinhold, W. Seichter, K. Köhnke, J. Seidel, E. Weber, *Adv. Mater.* **1997**, *9*, 958.

[23] A similar sorption experiment at 25 °C using chloroform instead of BU yielded an 1:1-inclusion stoichometry. A preliminary X-ray analytical study of a single crystal obtained from solution gave evidence that the same channel-type structure of BAOT is formed also in this case.

[24] G. J. Klap, S. M. van Klooster, M. Wübbenhorst, J. C. Jansen, H. van Bekkum, J. van Turnhout, *J. Phys. Chem. B* **1998**, *102*, 9518–9524.

[25] A. Quintel, J. Hulliger, M. Wübbenhorst, *J. Phys. Chem. B* **1998**, *102*, 4277–4283.

[26] J. Hulliger, *Z. Kristallogr.* **1999**, *214*, 9–13.

[27] a) O. König, H.-B. Bürgi, T. Armbruster, J. Hulliger, T. Weber, *J. Am. Chem. Soc.* **1997**, *119*, 10632–10640; b) K. D. H. Harris, P. E. Jupp, *Chem. Phys. Lett.* **1997**, *274*, 525–534.

[28] A. Quintel, S. W. Roth, J. Hulliger, M. Wübbenhorst, *Mol. Cryst. Liq. Cryst.* **1999**, in press.

[29] J. Hulliger, P. J. Langley, A. Quintel, P. Rechsteiner, S. W. Roth in *Supramolecular Engineering of Synthetic Metallic Materials*, *Vol. 518* (Eds.: J. Veciana, C. Rovira, D. B. Amabilina), NATOASI Ser. C, Kluwer, London, **1999**, pp. 67–81.

[30] Organikum, 20th ed, Johann Ambrosius Barth, Heidelberg, Leipzig, **1996**, 502.

[31] J. Hulliger, *Angew. Chem.* **1994**, *106,* 151–171; *Angew. Chem. Int. Ed. Engl.* **1994**, *33*, 143–162.

Received: June 21, 1999 [F 1863]